An integral approach to bedrock river profile analysis

An integral approach to bedrock river profile analysis

J. Taylor Perron and Leigh Royden

Department of Earth, Atmospheric and Planetary Sciences, Massachusetts Institute of Technology, Cambridge MA 02139

Abstract

Bedrock river profiles are often interpreted with the aid of slope-area analysis, but noisy topographic data make such interpretations challenging. We present an alternative approach based on an integration of the steady-state form of the stream power equation. The main component of this approach is a transformation of the horizontal coordinate that converts a steady-state river profile into a straight line with a slope that is simply related to the ratio of the uplift rate to the erodibility. The transformed profiles, called chi plots, have other useful properties, including co-linearity of steady-state tributaries with their main stem and the ease of identifying transient erosional signals. We illustrate these applications with analyses of river profiles extracted from digital topographic datasets.

Introduction

Bedrock rivers record information about a landscape's bedrock lithology, tectonic context, and climate history. It has become common practice to use bedrock river profiles to test for steady-state topography, infer deformation history, and calibrate erosion models (see reviews by Whipple, 2004, and Wobus et al., 2006). The most widely used models of bedrock river incision express the erosion rate in terms of channel slope and drainage area, which makes them easy to apply to topographic measurements and incorporate into landscape evolution models. We focus on the stream power equation:

$$\frac{\partial z}{\partial t} = U(x,t) - K(x,t) A(x,t)^m \left|\frac{\partial z}{\partial x}\right|^n \tag{1}$$

where z is elevation, t is time, x is horizontal upstream distance, U is the rate of rock uplift relative to a reference elevation, K is an erodibility coefficient, A is drainage area, and m and n are constants. Although equation (1) is commonly referred to as the stream power equation, it can be derived from the assumption that erosion rate scales with either stream power per unit area of the bed (Seidl and Dietrich, 1992; Howard et al., 1994) or bed shear stress (Howard and Kerby, 1983).

If the stream power equation is used to describe the evolution of a river profile, a common analytical approach is to assume a topographic steady state ($\partial z/\partial t = 0$) with uniform U and K and solve equation (1) for the channel slope:

$$\left|\frac{dz}{dx}\right| = \left(\frac{U}{K}\right)^{\frac{1}{n}} A(x)^{-\frac{m}{n}} \tag{2}$$

Equation (2) predicts a power-law relationship between slope and drainage area. If such a power law is observed for a given profile, it supports the steady state assumption, and the exponent and coefficient of a best-fit power law can be used to infer m/n and $(U/K)^{1/n}$, respectively. Alternatively, deviations from a power law slope-area relationship may be evidence of transient evolution of the river profile, variations in bedrock erodibility, or transitions to other dominant erosion and transport mechanisms (Whipple and Tucker, 1999; Tucker and Whipple, 2002; Stock et al., 2005).

Slope-area analysis has been widely applied to the study of bedrock river profiles (e.g., Flint, 1974; Tarboton et al., 1989; Wobus et al., 2006), but it suffers from significant limitations. Topographic data are subject to errors and uncertainty and are typically noisy. Estimates of slope obtained by differentiating a noisy elevation surface are even noisier. This typically causes considerable scatter in slope-area plots, which makes it challenging to identify a power-law trend with adequate certainty. Perhaps more concerning is the possibility that the scatter may obscure deviations from a simple power law that could indicate a change in process, a transient signal, or a failure of the stream power model. Another limitation of slope-area analysis is that the slope measured in a coarsely sampled topographic map may differ from the reach slope relevant to flow dynamics.

Strategies have been proposed to cope with some of these problems. In the common case of digital elevation maps (DEMs) that contain stair-step artefacts associated with the original contour source maps, for example, sampling at a regular and carefully selected elevation interval can extract the approximate points where the stream profile crosses the original contours (Wobus et al., 2006). This method requires care, however, and at best it reproduces the slopes that correspond to the original contours, which may be inaccurate. Measuring the slope over elevation intervals that correspond to long horizontal distances can compound the problem of measuring an average slope that differs from the local slope that drives flow. Furthermore, as Wobus et al. (2006) note, the contour sampling approach cannot distinguish between artefacts associated with the DEM generation procedure and real topographic features. Other common techniques for reducing noise and uncertainty in slope-area analyses include smoothing the river profile and logarithmic binning of slope measurements. Some of these approaches have been shown to yield good results (Wobus et al., 2006), but all introduce biases that are difficult to evaluate without field surveys.

In this paper, we propose a more robust method that alleviates many of these problems by avoiding measurements of channel slope. Our method uses elevation instead of slope as the dependent variable, and a spatial integral of drainage area as the independent variable. This approach has additional advantages that include the simultaneous use of main stem and tributaries to calibrate the stream power law, the ease of comparing profiles with different uplift rates, erosion parameters, or spatial scales, and clearer identification of transient signals. We present examples that demonstrate these advantages.

Transformation of river profiles

Change of horizontal coordinate

Our procedure is based on a change of the horizontal spatial coordinate of a river longitudinal profile. Separating variables in equation (2), assuming for generality that U and K may be spatially variable, and integrating yields

$$\int dz = \int \left(\frac{U(x)}{K(x)A(x)^m} \right)^{\frac{1}{n}} dx \quad . \tag{3}$$

Performing the integration in the upstream direction from a base level x_b to an observation point x yields an equation for the elevation profile:

$$z(x) = z(x_b) + \int_{x_b}^{x} \left(\frac{U(x)}{K(x)A(x)^m} \right)^{\frac{1}{n}} dx \quad . \tag{4}$$

There is no special significance associated with the choice of x_b; it is merely the downstream end of the portion of the profile being analysed. The integration can also be performed in the downstream direction, but it is best to use the upstream direction for reasons that will become apparent below.

Equation (4) applies to cases in which the profile is in steady state, but is spatially heterogeneous (if, for example, the profile crosses an active fault or spans different rock types, or if precipitation rate varies over the drainage basin). In the case of spatially invariant uplift rate and erodibility, the equation for the profile reduces to a simpler form,

$$z(x) = z(x_b) + \left(\frac{U}{K}\right)^{\frac{1}{n}} \int_{x_b}^{x} \frac{dx}{A(x)^{\frac{m}{n}}} \quad (5)$$

To create transformed river profiles with units of length on both axes, it is convenient to introduce a reference drainage area, A_0, such that the coefficient and integrand in the trailing term are dimensionless,

$$z(x) = z(x_b) + \left(\frac{U}{KA_0^m}\right)^{\frac{1}{n}} \chi \quad (6a)$$

with

$$\chi = \int_{x_b}^{x} \left(\frac{A_0}{A(x)}\right)^{\frac{m}{n}} dx \quad (6b)$$

Equation (6) has the form of a line in which the dependent variable is z and the independent variable is the integral quantity χ, which has units of distance. The z-intercept of the line is the elevation at x_b, and the dimensionless slope is $(U/K)^{1/n}/A_0^{m/n}$. We refer to a plot of z vs. χ for a river profile as a "chi plot."

The use of this coordinate transformation to linearize river profiles was originally proposed by Royden et al. (2000), and has subsequently been used to determine stream power parameters (Sorby and England, 2004; Harkins et al., 2007; Whipple et al., 2007). In this paper, we expand on this approach and explore additional applications of chi plots. As we show in the examples below, a chi plot can be useful even if U and K are spatially variable, or if the profile is not in steady state. The coordinate χ in equation (6) is also similar to the dimensionless horizontal coordinate χ in the analysis of Royden and Perron

(2012), which can be referred to for a more theoretical treatment of the stream power equation.

Measuring χ

It is usually not possible to evaluate the integral quantity χ in equation (6) analytically, but given a series of upslope drainage areas measured at discrete values of x along a stream profile, it is straightforward to approximate the value of χ at each point using the trapezoid rule or another suitable approximation. If the points along the profile are spaced at approximately equal intervals, the simplest approach is to calculate the cumulative sum of $[A_0/A(x)]^{m/n}$ along the profile in the upstream direction and multiply by the average distance between adjacent points. (Using the average distance avoids the "quantization" effect introduced by a steepest descent path through gridded data, in which point-to-point distances can only have values of δ or $\delta\sqrt{2}$, where δ is the grid resolution.) If δ varies significantly along the profile, or varies systematically with x, it is preferable to calculate the cumulative sum of $[A_0/A(x)]^{m/n}\delta(x)$. If desired, $\delta(x)$ can be smoothed with a moving average before performing the summation.

In most cases, the value of m/n required to compute χ will be unknown. In the next section, we illustrate a procedure for finding m/n that improves on conventional slope-area analysis.

Examples

Identifying steady-state profiles

The preceding analysis predicts that a steady-state bedrock river profile will have a linear chi plot. To demonstrate how the coordinate transformation can be used to identify a steady state river profile, we analysed the longitudinal profile of Cooskie Creek (Fig. 1a), one of several bedrock rivers in the Mendocino Triple Junction (MTJ) region of northern California studied previously by Merritts and Vincent (1989) and Snyder et al. (2000, 2003a,b). We determined upstream distance, elevation, and drainage area along the profile by applying a steepest descent algorithm to a DEM with 10 m grid spacing. For a range of m/n values ranging from 0 to 1, we calculated χ in equation (6), performed a linear least-squares regression of elevation against χ, and recorded the R^2 value as a measure of goodness of fit. A plot of R^2 against m/n (Fig. 1b) has a well-defined maximum at $m/n = 0.36$, implying that this is the best-fitting value. We then transformed the longitudinal profile according to equation (6) with $m/n = 0.36$ and $A_0 = 1$ km^2. The resulting chi plot (Fig. 1c) shows that the transformed profile closely follows a linear trend, suggesting that the profile is nearly in steady state. The slope of the regression line is 0.12, which, combined with an uplift rate of 3.5 mm/yr inferred from uplifted marine terraces (Merritts and Bull, 1989), implies an erodibility $K = 0.0002$ m$^{0.28}$/yr for $n = 1$. Note that the stair-step features in the longitudinal profile (Fig. 1a), which would produce considerable scatter in a slope-area plot, do not interfere with the regression analysis, and introduce only minor deviations from the linear trend in the chi plot of the transformed profile (Fig. 1c).

Using tributaries to estimate stream power parameters

A useful property of the coordinate transformation is that it scales points with similar elevations to similar values of χ, even if those points have different drainage areas. This implies that tributaries that are in steady state and that have the same uplift rate and erosion parameters as the main stem should be co-linear with the main stem in a chi plot. The co-linearity of tributaries and main stem provides a second, independent constraint on m/n: in theory, the correct value of m/n should both linearize all the profiles and collapse the tributaries and main stem to a single line. This highlights one reason for performing the integration in equation (3) in the upstream direction: tributaries have the same elevation as the main stem at their downstream ends, but not at their upstream ends.

Fig. 2 illustrates this principle with an analysis of Rush Run in the Allegheny Plateau of northern West Virginia. We extracted profiles of the main stem and nine tributaries of Rush Run from a DEM with 3 m grid spacing (Fig. 2a). The tributary longitudinal profiles differ from one another and from the main stem profile (Fig. 2b). Transforming the profiles with three different values of m/n (Fig. 2c-e) demonstrates how the best choice of m/n collapses the tributaries and main stem on a chi plot (Fig. 2d); for other values of m/n, the tributaries have systematically higher (Fig. 2c) or lower (Fig. 2e) elevations than the main stem in transformed coordinates.

In practice, the value of m/n that best collapses the tributaries and main stem is not always the value that maximizes the linearity of each individual profile. In the case of Rush Run, the value of $m/n = 0.65$ that best collapses the tributaries makes the main stem slightly concave down in transformed coordinates (Fig. 2d). Provided there are no systematic differences in erodibility or precipitation rates between the main stem and tributaries, this minor discrepancy may be an indication that the drainage basin is slightly out of equilibrium. Alternatively, it could be an indication that the mechanics of channel incision are not completely described by the stream power equation. This example illustrates how the comparison of transformed tributary and main stem profiles can provide a perspective on drainage basin evolution that would be difficult to attain with slope-area analysis.

Comparisons among profiles

Another common application of river profile analysis is to identify topographic differences among rivers that are thought to experience different uplift or precipitation rates or that have eroded through different rock types (e.g., Kirby and Whipple, 2001; Kirby et al., 2003). These effects are modelled by the uplift rate U and the erodibility coefficient K. The coefficient of the power law in equation (2), which includes the ratio of these two parameters, is often referred to as a steepness index, because, all else being equal, the steady-state relief of the river profile is higher when U/K is larger. The steepness index is usually determined from the intercept of a linear fit to log-transformed slope and area data. The uncertainty in this intercept can be substantial due to scatter in the slope-area data (Harkins et al., 2007). In our coordinate transformation, the steepness index is simply the slope of the transformed profile, $dz/d\chi$, which provides a means of estimating U/K that is less subject to uncertainty (Royden et al., 2000; Sorby and England, 2004; Harkins et al., 2007; Whipple et al., 2007) as well as an intuitive visual assessment of differences among profiles.

To illustrate this point, we analysed 18 of the profiles from the MTJ region studied by Snyder et al. (2000) (Fig. 3a). The profiles span an inferred increase in uplift rate northward along the coast from roughly 0.5 mm/yr to roughly 4 mm/yr associated with the passage of the Mendocino Triple Junction (Fig. 3c; Merritts and Bull, 1989; Merritts and Vincent, 1989; Merritts, 1996). The topographic data and procedures were the same as in the Cooskie Creek example. We determined the best-fitting value of m/n for each profile with the approach in Fig. 1b, and found a mean m/n of 0.46 ± 0.11 (s.d.).

When comparing the steepness of transformed profiles, it is important to use the same values of A_0 and m/n to calculate χ. We therefore transformed all the profiles using $A_0 = 1$ km^2 and $m/n = 0.46$ (Fig. 1b). The goodness of linear fits to the profiles using this mean value of m/n (average R^2 of 0.992) is nearly as good as when using the best-fitting m/n for each profile (average R^2 of 0.995). (Note that these measures of R^2 are inflated by serially correlated residuals – see Discussion section – but the comparison of their relative values is valid.) With the profiles' concavity largely removed by the transformation, the effect of uplift rate on profile steepness (the slopes of the profiles in

Fig. 3b) is very apparent, whereas a very careful slope-area analysis is required to resolve the steepness difference due to the noise in the elevation data (compare to Fig. 4 of Wobus et al. (2006)).

The analysis in Fig. 3 also supports the conclusion of Snyder et al. (2000) that the difference in steepness between the profiles in the zones of fast uplift (red profiles in Fig. 3b) and slower uplift (blue profiles in Fig. 3b) is less than expected if only uplift rate differs between these two zones. The dimensionless slope of the transformed profiles is 0.21 ± 0.06 (mean ± s.d.) for those inferred to be experiencing uplift rates of 3 to 4 mm/yr and 0.13 ± 0.01 for those inferred to be experiencing uplift rates of 0.5 mm/yr, a slope ratio of only 1.62 ± 0.48 for a six- to eight-fold difference in uplift rate. If these uplift rates are correct, and if n is less than ~2, as is typically inferred (Howard and Kerby, 1983; Seidl and Dietrich, 1992; Seidl et al., 1994; Rosenbloom and Anderson, 1994; Stock and Montgomery, 1999; Whipple et al., 2000; van der Beek and Bishop, 2003), there must be other differences among the profiles that affect the steepness. Given the inferred uniformity of the lithology in the MTJ region (Snyder et al., 2003a, and references therein), one possible explanation is that increased rainfall and associated changes in weathering and erosion mechanisms have elevated the erodibility, K, in the zone of faster uplift and higher relief (Snyder et al., 2000, 2003a,b).

The importance of variables other than uplift rate is most apparent in the chi plots of Fourmile and Cooskie Creeks (orange profiles in Fig. 3b). These rivers have only slightly slower inferred uplift rates than the red profiles in Fig. 3b, but they have much gentler slopes. In fact, their slopes are comparable to those of the blue profiles in the slower uplift zone. A possible explanation for this discrepancy is that local structural deformation has rendered the bedrock more easily erodible in the Cooskie Shear Zone. Whatever the reason for the reduced effect of uplift rate on profile steepness, this example from the MTJ region demonstrates the ease of comparisons between transformed river profiles believed to be in steady state with respect to different erosion parameters or rates of tectonic forcing.

Transient signals

Even if a river is not in a topographic steady state, a chi plot of its longitudinal profile can be useful. Just as transformed tributaries plot co-linearly with a transformed main stem, transient signals with a common origin, propagating upstream through different channels, plot in the same location in transformed coordinates (χ and z). Whipple and Tucker (1999) noted that transient signals in river profiles governed by the stream power equation propagate vertically at a constant rate, and exploited this property to calculate timescales for transient adjustment of profiles in response to a step change in K or U. The transformation presented in this paper removes the effect of drainage area, and therefore shifts the transient signals in the profiles to the same horizontal position (χ), provided that K and U are uniform.

We illustrate this property with an example from the Big Tujunga drainage basin in the San Gabriel Mountains of southern California (Fig. 4a), where Wobus et al. (2006) observed an apparent transient signal in multiple tributaries within the basin. Longitudinal profiles (Fig. 4b) reveal steep reaches in the main stem and some tributaries at elevations of roughly 900-1000 m but different streamwise positions. Differences in drainage basin size and shape make it difficult to compare the profiles and determine if and how these features are related. Transforming the profiles using $m/n = 0.4$, the value that best collapses the tributaries to the main stem and linearizes the profiles, clarifies the situation (Fig. 4c). The steep sections of the transformed profiles plot in nearly the same location. The transformed profiles also have a systematically steeper slope downstream of this knick point than upstream, suggesting an increase in uplift rate, the preferred interpretation of Wobus et al. (2006), or a reduction in erodibility. It is difficult to tell whether the knick point is stationary or migrating (Royden and Perron, 2012), but the lack of an obvious fault or lithologic contact suggests that it may be a transient signal that originated downstream of the confluence of the analysed profiles and has propagated upstream to varying extents.

The horizontal overlap of the steep sections in the chi plot in Fig. 3c is compelling, but it is not perfect. The residual offsets may have arisen from spatial variability in channel incision processes, precipitation, or bedrock erodibility. This difference, which is not obvious in the original longitudinal profiles (Fig. 3b) and would probably not be apparent in a slope-area plot, highlights the sensitivity of the coordinate transformation technique.

Discussion

Advantages of the integral approach to river profile analysis

The approach described in this paper has several advantages over slope-area analysis. The most significant advantage is that it obviates the need to calculate slope from noisy topographic data. This makes it possible to perform useful analyses with elevation data that would ordinarily be avoided. The landscape in Fig. 2, for example, has sufficiently low relief that even elevation data derived from laser altimetry contains enough noise to frustrate a slope-area analysis, but the transformed profiles are relatively easy to interpret.

The reduced scatter relative to slope-area plots provides better constraints on stream power parameters estimated from topographic data. In addition, a chi plot can potentially provide an independent constraint on both m/n and U/K, because the profile fits are constrained two ways: by the requirement to linearize individual profiles (Fig. 1), and by the requirement to align tributaries with the main stem (Fig. 2). Although steady state tributary and main stem channels should also be co-linear on a logarithmic slope-area plot, they typically have different drainage areas, and therefore do not usually overlap. In contrast, the integral method produces transformed longitudinal profiles with overlapping chi coordinates, making it easier to visually assess the match between tributaries and main stem.

Removing the effect of drainage area through this coordinate transformation makes it possible to compare river profiles independent of their spatial scale. This is useful both for comparing different drainage basins (Fig. 3) and for comparing channels within a drainage basin (Fig. 4). Transient erosional features, such as knick points, that originated from a common source should plot at the same value of χ in all affected channels (Fig. 4). Transient features are also easier to identify in a chi plot because it is easy to see departures from a linear trend with relatively little noise. Similarly, transformed profiles should accentuate transitions from bedrock channels to other process zones within the fluvial network, such as channels in which elevation changes are dominated by alluvial sediment transport or colluvial processes and debris flows (Whipple and Tucker, 1999; Tucker and Whipple, 2002; Stock et al., 2005).

Finally, the coordinate transformation presented here is compatible with the analytical solutions of Royden and Perron (2012), which aid in understanding the transient evolution of river profiles governed by the stream power equation. As noted above, the integral quantity χ in equation (6) is similar to the dimensionless horizontal coordinate χ used by Royden and Perron (2012) to derive analytical solutions for profiles adjusting to spatial and temporal changes in uplift rate, erodibility, or precipitation. (For uniform K, as is assumed in this paper, it is linearly proportional to their χ.) River profiles transformed according to equation (6) can easily be compared with these solutions to investigate possible scenarios of transient profile evolution.

Disadvantages of the integral approach

The main disadvantage of the integral approach is that the coordinate transformation requires knowledge of m/n, which is usually not known *a priori*. However, we have demonstrated a simple iterative approach for finding the best-fitting value of m/n that is easy to implement (Fig. 1b). Moreover, the dependence of the transformation on m/n provides an additional constraint on m/n, the co-linearity of main stem and tributaries, which is not available in slope-area analysis.

Another drawback of the integral method is that chi plots, like slope-area plots, do not account for variations on, or inadequacy of, the stream power/shear stress model. Multiple studies have found that effects not included in equation (1), including erosion thresholds (e.g., Snyder et al., 2003b; DiBiase and Whipple, 2011), discharge variability (e.g., Snyder et al., 2003b; Lague et al., 2005; DiBiase and Whipple, 2011) and abrasion and cover by sediment (e.g., Whipple and Tucker, 2002; Turowski et al. 2007), can influence the longitudinal profiles of bedrock rivers. It may be possible to use an integral approach to derive definitions of χ for channel incision models that include these effects, but such an analysis is beyond the scope of this paper.

The form of the integral method presented here can, however, help to identify profiles that are not adequately described by equation (1), because their chi plots should be non-linear. Given the larger uncertainties in slope-area analyses, it is possible that some profiles have incorrectly been identified as steady state, or otherwise consistent with the stream power equation, with deviations from the model prediction concealed by the scatter in the slope-area data. The integral method, which is less susceptible to noise in elevation data, is a more sensitive tool for identifying such deviations.

Evaluating uncertainty

The transformation of river longitudinal profiles into linear profiles with little scatter raises the question of how to estimate the uncertainty in stream power parameters determined from topographic data. The most obvious approach is to use the uncertainties obtained by fitting a model to an individual profile. Slope-area analysis of steady-state profiles is appealing from this standpoint, because a least-squares linear regression of log-transformed slope-area data provides an easy way of estimating the uncertainty in m/n (the slope of the regression line) and $(U/K)^{1/n}$ (the intercept). However, the resulting uncertainties mostly describe how precisely one can measure slope, not how precisely the parameters are known for a given landscape.

The integral method presented in this paper makes this distinction more apparent. For example, when the profile of Cooskie Creek in Fig. 1a is transformed with the best-fitting value of m/n, there is a very small uncertainty (0.2% standard error) in the slope of the best linear fit (Fig. 1c), but this small uncertainty surely overestimates the precision with which $(U/K)^{1/n}$ can be measured for the bedrock rivers of the King Range. Statistically, this uncertainty in the slope of the regression line is also an underestimate because the transformed profile is a continuous curve, and therefore the residuals of the linear fit are serially correlated. This property of the data does not bias the regression coefficients,

$z(x_b)$ and $(U/K)^{1/n}/A_0^{m/n}$, but it does lead to underestimates of their uncertainties. Thus, if a chi plot is used to estimate the uncertainty of stream power parameters by fitting a line to a single river profile, a procedure for regression with autocorrelated residuals must be used (e.g., Kirchner, 2001).

There are better ways to estimate uncertainty in stream power parameters. One, which can be applied to either slope-area analysis or the integral method, is to make multiple independent measurements of different river profiles. This was the approach used to estimate the uncertainty in steepness within each uplift zone in the MTJ region example. The standard errors of the mean steepness among profiles within the fast uplift zone (8.6%) and the slower uplift zone (3.4%) are considerably larger than the standard errors of steepness for individual profiles. If it is possible to measure multiple profiles that are believed to be geologically similar, this approach provides estimates of uncertainty that are more meaningful than the uncertainty in the fit to any one profile. Alternatively, if only one drainage basin is analysed, the integral method provides a new means of estimating the uncertainty in m/n: comparing the value that best linearizes the main stem profile (Fig. 1c) with the value that maximizes the co-linearity of the main stem with its tributaries (Fig. 2c-e).

Conclusions

We have described a simple procedure that makes bedrock river profiles easier to interpret than in slope-area analysis. The procedure eliminates the need to measure channel slope from noisy topographic data, linearizes steady-state profiles, makes steady-state tributaries co-linear with their main stem, and collapses transient erosional signals with a common origin. The procedure is well suited to analysing both steady state and transient profiles, and is useful for interpreting the lithology, tectonic histories, and climate histories of river profiles, even from coarse or imprecise topographic data.

Acknowledgments

We thank Kelin Whipple for helpful discussions and for stimulating our interest in river profiles. This study was supported by the NSF Geomorphology and Land-use Dynamics Program under award EAR-0951672 to J.T.P. and by the Continental Dynamics Program under award EAR-0003571 to L.R. Comments by two anonymous referees helped us improve the paper.

References

DiBiase, R. A., and K. X. Whipple (2011), The influence of erosion thresholds and runoff variability on the relationships among topography, climate, and erosion rate, *J. Geophys. Res.*, 116, F04036, doi:10.1029/2011JF002095.

Flint, J. J. (1974), Stream gradient as a function of order, magnitude and discharge, *Water Resour. Res.*, 10(5), 969-973.

Harkins, N., E. Kirby, A. Heimsath, R. Robinson, and U. Reiser (2007), Transient fluvial incision in the headwaters of the Yellow River, northeastern Tibet, China, *J. Geophys. Res.*, 112, F03S04, doi:10.1029/2006JF000570.

Howard, A. D., W. E. Dietrich, and M. A. Seidl (1994), Modeling fluvial erosion on regional to continental scales, *J. Geophys. Res.*, *99*(B7), 13,971–13,986.

Howard, A. D. and G. Kerby (1983), Channel changes in badlands, *Bull. Geol. Soc. Am.*, *94*(6), 739–752.

Kirby, E. and K. X. Whipple (2001), Quantifying differential rock-uplift rates via stream profile analysis, *Geology*, 29, 415-418.

Kirby, E., K. X. Whipple, W. Tang and Z. Chen (2003), Distribution of active rock uplift along the eastern margin of the Tibetan Plateau: Inferences from bedrock river profiles, *Journal of Geophys. Res.*, 108, 2217, doi:10.1029/2001JB000861.

Kirchner, J. W. (2001), Data Analysis Toolkit #11: Serial Correlation, course notes from EPS 120: Analysis of Environmental Data, U. C. Berkeley, retrieved from http://seismo.berkeley.edu/~kirchner/eps_120/EPSToolkits.htm on May 20, 2012.

Lague, D., N. Hovius, and P. Davy (2005), Discharge, discharge variability, and the bedrock channel profile, *J. Geophys. Res.*, 110, F04006, doi:10.1029/2004JF000259.

Merritts, D. J. (1996), The Mendocino triple junction: Active faults, episodic coastal emergence, and rapid uplift, *J. Geophys. Res.*, 101(B3), 6051–6070, doi:10.1029/95JB01816.

Merritts, D., and K.R. Vincent (1989), Geomorphic response of coastal streams to low, intermediate, and high rates of uplift, Medocino triple junction region, northern California, *Geological Society of America Bulletin*, *101*(11), 1373–1388.

Merritts, D., and W. B. Bull (1989), Interpreting Quaternary uplift rates at the Mendocino triple junction, northern California, from uplifted marine terraces, *Geology*, *17*(11), 1020–1024.

Rosenbloom, N. A., and R. S. Anderson (1994), Hillslope and channel evolution in a marine terraced landscape, Santa Cruz, California, *J. Geophys. Res.*, *99*(B7), 14,013–14,029.

Royden, L. H., M. K. Clark and K. X. Whipple (2000), Evolution of river elevation profiles by bedrock incision: Analytical solutions for transient river profiles related to changing uplift and precipitation rates, *EOS, Trans. American Geophysical Union,* 81, Fall Meeting Suppl., Abstract T62F-09.

Royden, L. and J. T. Perron (2012), Solutions of the stream power equation and application to the evolution of river longitudinal profiles, submitted to *J. Geophys. Res.*

Seidl, M. A., and W. E. Dietrich (1992), The problem of channel erosion into bedrock, *Catena*, *23*(D24), 101–124.

Seidl, M. A., W. E. Dietrich, and J. W. Kirchner (1994), Longitudinal profile development into bedrock: an analysis of Hawaiian channels, *J. Geol.*, *102*(4), 457–474.

Sorby, A. P. and P. C. England (2004), Critical assessment of quantitative geomorphology in the footwall of active normal faults, Basin and Range province, western USA, *EOS, Trans. American Geophysical Union,* 85, Fall Meeting Suppl., Abstract T42B-02.

Snyder, N. P., K. X. Whipple, G. E. Tucker, and D. J. Merritts (2000), Landscape response to tectonic forcing: Digital elevation model analysis of stream profiles in the Mendocino triple junction region, northern California, *GSA Bulletin*, *112*(8), 1250–1263.

Snyder, N. P., K. X. Whipple, G. E. Tucker, and D. J. Merritts (2003a), Channel response to tectonic forcing: field analysis of stream morphology and hydrology in the Mendocino triple junction region, northern California, *Geomorphology*, 53(1-2), 97-127.

Snyder, N. P., K. X. Whipple, G. E. Tucker, and D. J. Merritts (2003b), Importance of a stochastic distribution of floods and erosion thresholds in the bedrock river incision problem, *J. Geophys. Res.*, 108(B2), 2117, doi:10.1029/2001JB001655.

Stock, J. D. and D. R. Montgomery (1999), Geologic constraints on bedrock river incision using the stream power law, *J. Geophys. Res.*, *104*(B3), 4983–4994.

Stock, J. D., D. R. Montgomery, B. D. Collins, W. E. Dietrich, and L. Sklar (2005), Field measurements of incision rates following bedrock exposure: Implications for process controls on the long profiles of valleys cut by rivers and debris flows, *Geol. Soc. Am. Bull.*, 117, 174–194.

Tarboton, D., R. L. Bras and I. Rodríguez-Iturbe (1989), Scaling and elevation in river networks, *Water Res. Res.*, 25(9), 2037–2051.

Turowski, J. M., D. Lague, and N. Hovius (2007), Cover effect in bedrock abrasion: A new derivation and its implications for the modeling of bedrock channel morphology, Journal of Geophysical Research-Earth Surface, 112, F04006, doi:10.1029/2006JF000697.

van der Beek, P. and P. Bishop (2003), Cenozoic river profile development in the upper Lachlan catchment (SE Australia) as a test of quantitative fluvial incision models, *J. Geophys. Res.* 108, 2309, doi:10.1029/2002JB002125.

Whipple, K. X., and G. E. Tucker (1999), Dynamics of the stream-power river incision model: Implications for height limits of mountain ranges, landscape response timescales, and research needs, *J. Geophys. Res.*, *104*(B8), 17661–17674.

Whipple, K. X., G. S. Hancock and R. S. Anderson (2000), River incision into bedrock: Mechanics and relative efficacy of plucking, abrasion, and cavitation, *Geol. Soc. Am. Bull.*, 112, 490–503.

Whipple, K. X., and G. E. Tucker (2002), Implications of sediment-flux-dependent river incision models for landscape evolution, *J. Geophys. Res.*, 107 (B2), 2039, doi:10.1029/2000JB000044.

Whipple, K. X. (2004), Bedrock rivers and the geomorphology of active orogens, *Annu. Rev. Earth Planet. Sci.*, *32*(1), 151–185.

Whipple, K. X., C. Wobus, E. Kirby, B. Crosby and D. Sheehan (2007), New Tools for Quantitative Geomorphology: Extraction and Interpretation of Stream Profiles from

Digital Topographic Data, Short Course presented at Geological Society of America Annual Meeting, Denver, CO. Available at http://www.geomorphtools.org.

Wobus, C., K.X. Whipple, E. Kirby, N. Snyder, J. Johnson, K. Spyropolou, B. Crosby and D. Sheehan (2006), Tectonics from topography: Procedures, promise, and pitfalls, *in* Willett, S.D., Hovius, N., Brandon, M.T., and Fisher, D.M., eds., *Tectonics, Climate, and Landscape Evolution*, Geological Society of America Special Paper 398, Penrose Conference Series, 55–74.

Figure Captions

Figure 1. Profile analysis of Cooskie Creek in the northern California King Range, USA. (a) Longitudinal profile of the bedrock section of the Creek, as determined by Snyder et al. (2000), extracted from the 1/3 arcsecond (approximately 10 m) U. S. National Elevation Dataset using a steepest descent algorithm. (b) R^2 statistic as a function of m/n for least-squares regression based on equation (6). The maximum value of R^2, which corresponds to the best linear fit, occurs at $m/n = 0.36$. (c) Chi plot of the longitudinal profile (black line), transformed according to equation (6) with $A_0 = 1$ km^2, compared with the regression line for $m/n = 0.36$ (gray line). If the stream power equation is valid and the uplift rate U and erodibility coefficient K are spatially uniform, the slope of the regression line is $(U/K)^{1/n}/A_0^{m/n}$.

Figure 2. Rush Run drainage basin in the Allegheny Plateau of northern West Virginia, USA. (a) Shaded relief map with black line tracing the main stem and gray lines tracing nine tributaries. Digital elevation data are from the 1/9 arcsecond (approximately 3 m) U.S. National Elevation Dataset. UTM zone 17 N. (b) Longitudinal profiles of the main stem (black line) and tributaries (gray lines). (c-e) Chi plots of longitudinal profiles, transformed according to equation (6), using $A_0 = 10$ km^2 and (c) $m/n = 0.55$, (d) $m/n = 0.65$, (e) $m/n = 0.75$.

Figure 3. River profiles in the Mendocino Triple Junction region of northern California, USA. (a) Shaded relief map showing locations of bedrock sections of the channels, as determined by Snyder et al. (2000), extracted from the 1/3 arcsecond (approximately 10 m) National Elevation Dataset. Blue profiles have slower uplift rates, red profiles have faster uplift rates, and orange profiles have faster uplift rates but are located in the Cooskie Shear Zone. (b) Chi plot of longitudinal profiles transformed according to equation (6), using $A_0 = 1$ km^2 and $m/n = 0.46$, the mean of the best-fitting values for all the profiles. Profiles have been shifted so that their downstream ends are evenly spaced along the horizontal axis. Elevation is measured relative to the downstream end of the bedrock section of each profile. (c) Uplift rate at the

location of each drainage basin, inferred from dating of marine terraces (Merritts and Bull, 1989; Merritts and Vincent, 1989; Snyder et al., 2000).

Figure 4. Big Tujunga drainage basin in the San Gabriel Mountains of California, USA. (a) Shaded relief map with black line tracing the main stem and gray lines tracing seven tributaries. Digital elevation data are from the 1/3 arcsecond (approximately 10 m) U.S. National Elevation Dataset. UTM zone 11 N. (b) Longitudinal profiles of the main stem (black line) and tributaries (gray lines). The gap in the main stem is the location of Big Tujunga Dam and Reservoir. (c) Chi plot of longitudinal profiles, transformed according to equation (6), using A_0 = 10 km^2 and m/n = 0.4, illustrating the approximate co-linearity of the tributaries and main stem despite the fact that the profiles do not appear to be in steady state with respect to uniform erodibility and uplift. Two straight dashed segments with different slopes are shown for comparison.

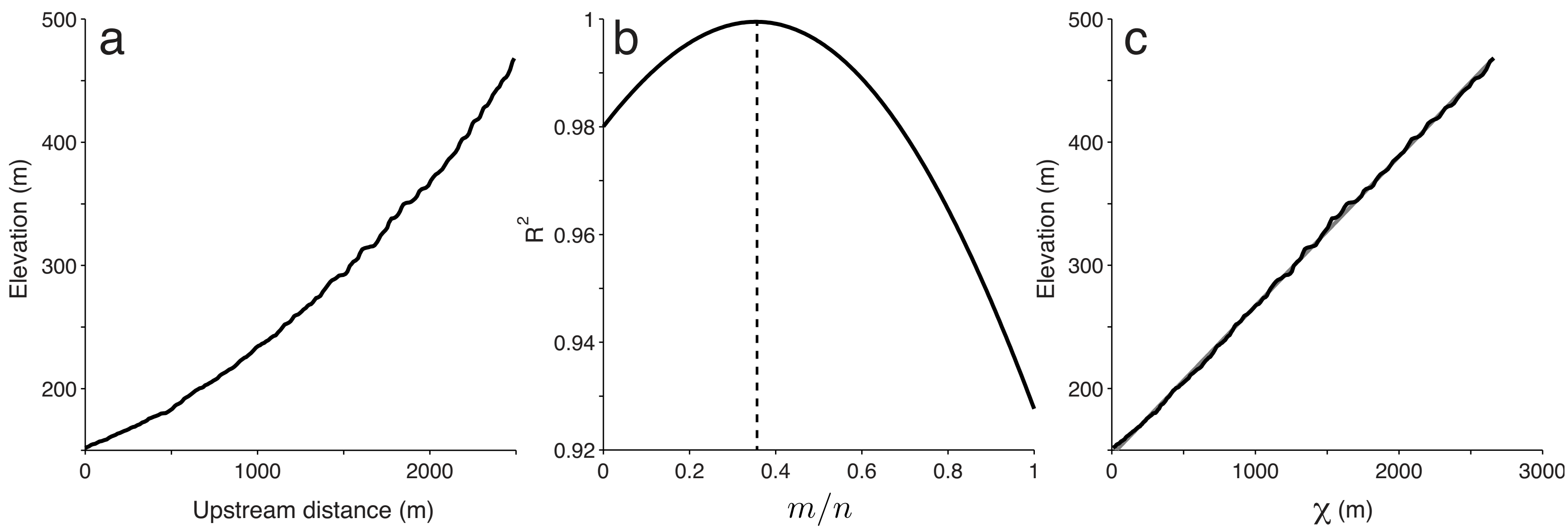
a
Elevation (m)
500
400
300
200
0
1000
2000
Upstream distance (m)
b
R^2
1
0.98
0.96
0.94
0.92
0
0.2
0.4
0.6
0.8
1
m/n
c
Elevation (m)
500
400
300
200
0
1000
2000
3000
χ (m)

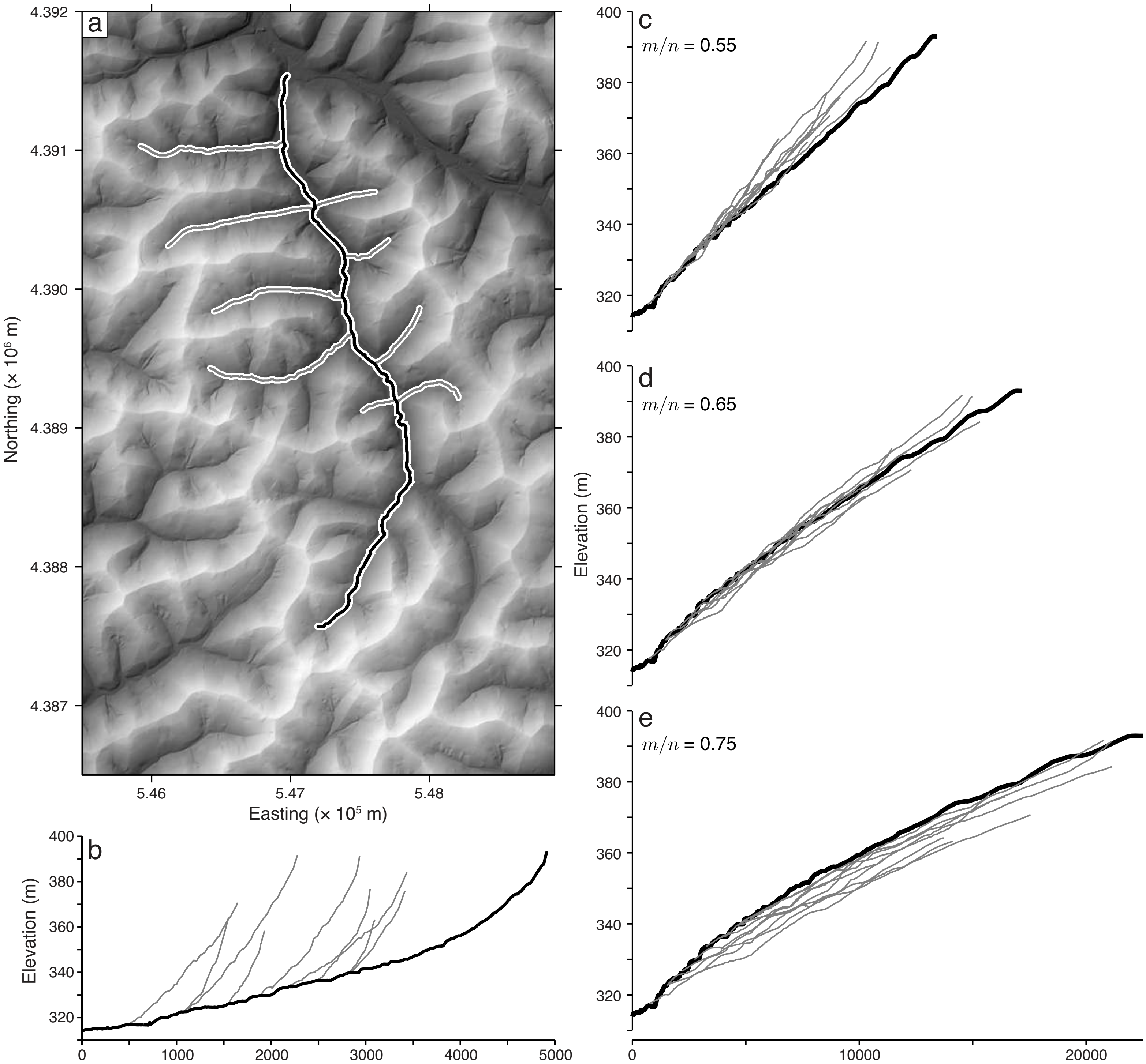
a
b
c
d
e
Northing (× 10^6 m)
Easting (× 10^5 m)
4.392
4.391
4.390
4.389
4.388
4.387
5.46
5.47
5.48
Elevation (m)
Upstream distance (m)
0
1000
2000
3000
4000
5000
320
340
360
380
400
m/n = 0.55
m/n = 0.65
m/n = 0.75
χ (m)
10000
20000

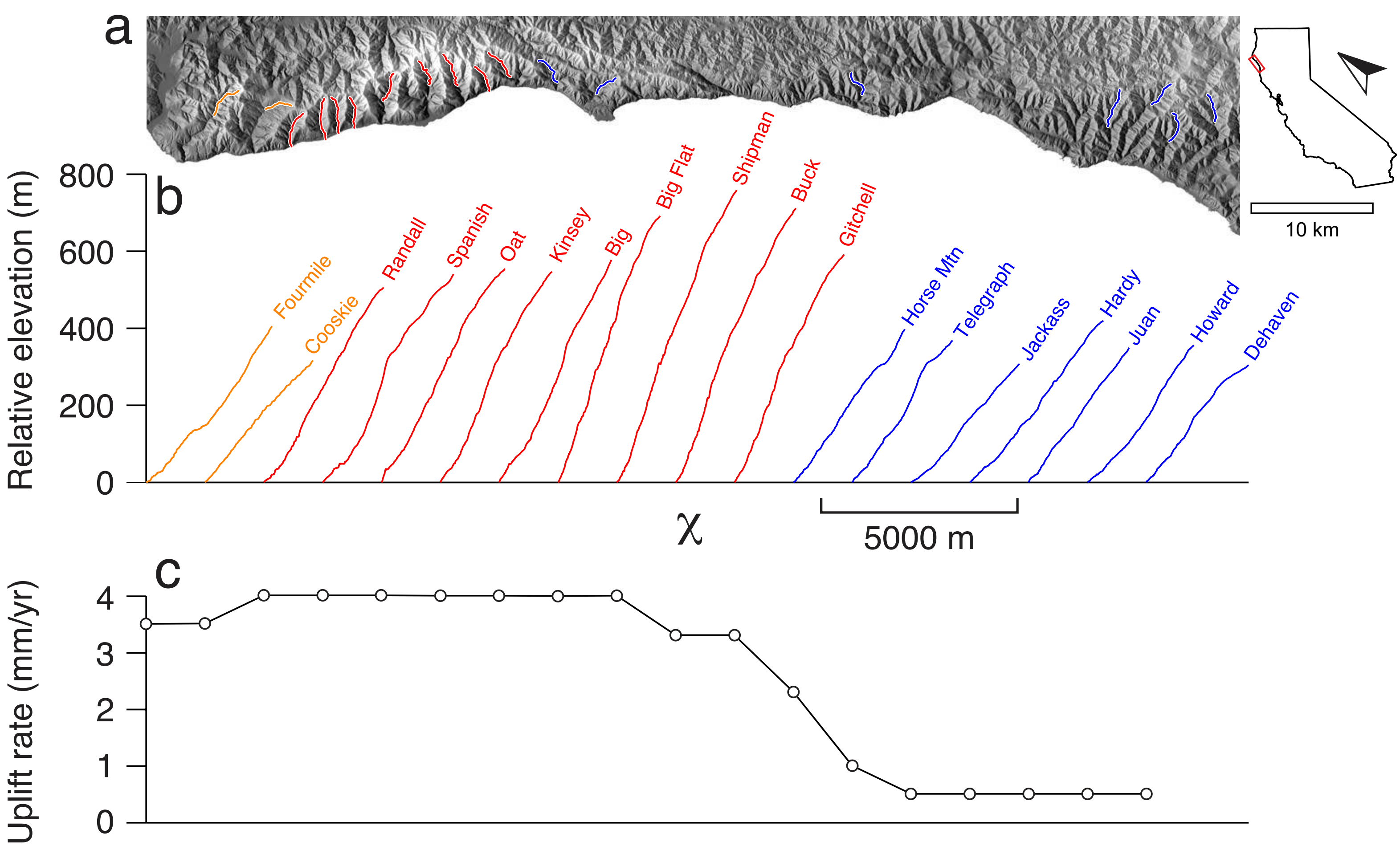

a
10 km
b
Relative elevation (m)
800
600
400
200
0
Fourmile
Cooskie
Randall
Spanish
Oat
Kinsey
Big
Big Flat
Shipman
Buck
Gitchell
Horse Mtn
Telegraph
Jackass
Hardy
Juan
Howard
Dehaven
χ
5000 m
c
Uplift rate (mm/yr)
4
3
2
1
0

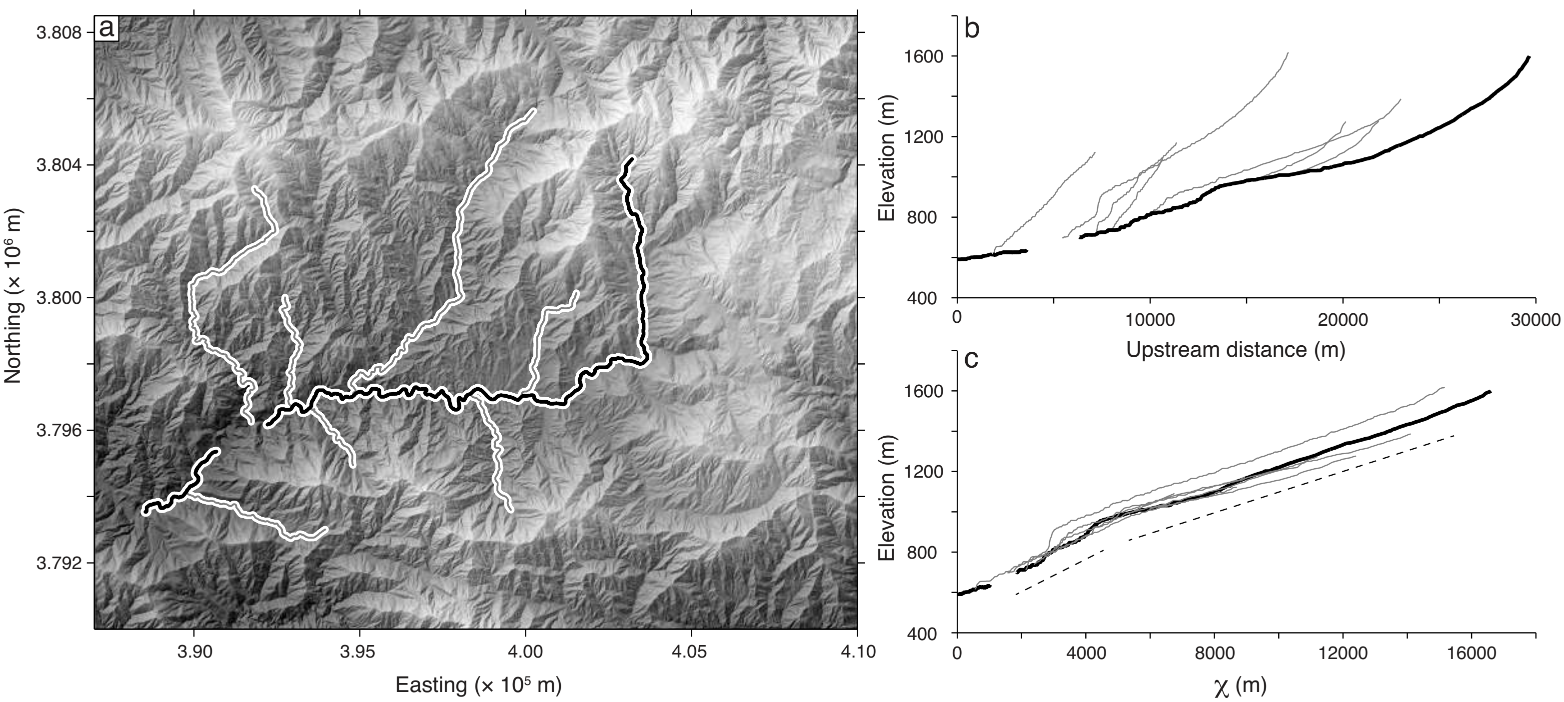

a
3.808
3.804
3.800
3.796
3.792
Northing (× 10⁶ m)
3.90
3.95
4.00
4.05
4.10
Easting (× 10⁵ m)
b
Elevation (m)
1600
1200
800
400
0
10000
20000
30000
Upstream distance (m)
c
Elevation (m)
1600
1200
800
400
0
4000
8000
12000
16000
χ (m)